The Chemistry of the Hydrazido(1−)-ligand. Preparations and Crystal Structures of $[Mo(NHNHCO_2Me)(NNCO_2Me)(S_2CNMe_2)_2]$, $[Mo(NHNMePh)(NNMePh)(S_2CNMe_2)_2]BPh_4$, and $[ReCl_2(NHNHCOPh)(NNHCOPh)(PPh_3)_2]$.‡ Mechanism of Formation of Substituted Hydrazines from $[Mo(NNRPh)_2(S_2CNMe_2)_2]$ (R = Me or Ph)

Jonathan R. Dilworth*,† and Richard A. Henderson
AFRC Unit of Nitrogen Fixation, University of Sussex, Brighton BN1 9RQ
Phillip Dahlstrom, Terrence Nicholson, and Jon A. Zubieta
State University of New York at Albany, Albany, NY 12222, U.S.A.

The preparation of three complexes containing a hydrazido(1−)-ligand is described, together with a kinetic study of the intermediacy of such a species in the hydrazine-forming reaction of acid with $[Mo(NNRPh)_2(S_2CNR'_2)_2]$ (R = R' = Me; R = Ph, R' = Et). Addition of 1 equivalent of HCl to $[Mo(NNMePh)_2(S_2CNMe_2)_2]$ gives $[Mo(NHNMePh)(NNMePh)(S_2CNMe_2)_2]^+$ isolated as its BPh_4^- salt [crystal data: space group $P2_1/n$, a = 16.102(3), b = 15.669(5), c = 18.752(2) Å, α = 90.00, β = 112.23(1), γ = 90.00°, Z = 4; 3 060 independent reflections gave an R value of 0.051]. Crystal data for $[Mo(NHNHCO_2Me)(N_2CO_2Me)(S_2CNMe_2)_2]$, space group $C2/c$, a = 19.963(1), b = 18.855(1), c = 13.127(1) Å, $\alpha = \gamma$ = 90.0, β = 114.41(1)°, Z = 8; 1 585 independent reflections gave R 0.066. Both complexes show distorted pentagonal-bipyramidal geometries with an NN'-bonded hydrazido(1−)-ligand in the pseudo-pentagonal plane. Reaction of $[ReCl_2(N_2COPh)(PPh_3)_2]$ with benzoylhydrazine gives $[ReCl_2(NHNHCOPh)(NNHCOPh)(PPh_3)_2]$ [crystal data: space group $P\bar{1}$, a = 12.276(2), b = 14.147(2), c = 15.284(2) Å, α = 86.33(1), β = 72.04(1), γ = 83.10(1)°, Z = 2; 4 995 independent reflections gave R 0.042]. Initial protonation of $[Mo(NNRPh)_2(S_2CNR'_2)_2]$ by HX (X = Cl or Br) gives $[Mo(NHNRPh)(NNRPh)(S_2CNR'_2)_2]^+$. Then, depending on R, ring closure occurs to give $[Mo(NHNRPh)(NNRPh)(S_2CNR'_2)_2]^+$ which competes with further protonation to give $[Mo(NHNHRPh)(NNRPh)(S_2CNR'_2)_2]^{2+}$. Solvent attack on the latter, followed by halide substitution, leads to further protonation of the hydrazide ligand leading to loss of hydrazinium salt and formation of $[MoX_2(NNRPh)(S_2CNR'_2)_2]$. The complex $[Mo(NHNRPh)(NNRPh)(S_2CNR'_2)_2]^+$ undergoes ring opening at too slow a rate for it to be an intermediate *en route* to hydrazine formation in excess of acid. The kinetics of the reactions of $[Mo(NHNRPh)(NNRPh)(S_2CNR'_2)_2]^+$ with a variety of bases suggests the formation of the transient NN'-bonded hydrazido(2−)-complex $[Mo(NNRPh)(NNRPh)(S_2CNR'_2)_2]$ (R' = R = Me) prior to regeneration of the bis[hydrazido(2−)]-complex.

Hydrazido(2−)-species have been identified as intermediates in the conversion of ligated dinitrogen into ammonia and also postulated to be involved in enzymatic nitrogen fixation.[1,2] Although many details of the alkylation [3,4] and protonation [5–7] of the complexes $[M(N_2)_2(PR_3)_4]$ (M = Mo or W, PR_3 = PMe_2Ph or ½ $Ph_2PCH_2CH_2PPh_2$) have been established, little is known about how hydrazido(2−)-species are converted into hydrazine or ammonia. In this paper we describe the synthesis and structural characterisation of a number of hydrazido(1−)-complexes which show a side-on mode of coordination, together with mechanistic studies of the intermediacy of such species in the protonation of hydrazido(2−)-ligands to hydrazine.

† *Present address:* Chemistry Department, University of Essex, Colchester C04 3SQ.

‡ Bis(dimethyldithiocarbamato)(*N'*-methoxycarbonyldiazenido-*N*)-[*N'*-methoxycarbonylhydrazido(1−)-*NN'*]molybdenum(IV), bis(dimethyldithiocarbamato)[*N'*-methyl-*N'*-phenylhydrazido(1−)-*NN'*]-[*N'*-methyl-*N'*-phenylhydrazido(2−)-*N*]molybdenum(VI) tetraphenylborate, and [*N'*-benzoylhydrazido(1−)-*N*][*N'*-benzoylhydrazido(2−)-*N*]dichlorobis(triphenylphosphine)rhenium(V).

Supplementary data available: see Instructions for Authors, *J. Chem. Soc., Dalton Trans.*, 1987, Issue 1, pp. xvii—xx.

Results

Preparation and Properties of Hydrazido(1−)-complexes.— The synthesis of the complexes $[Mo(NNRPh)_2(S_2CNR'_2)_2]$ (R = Me or Ph, R' = Me or Et) has been described in detail in an earlier publication.[8] The bis(hydrazido)-complexes react with an excess of acid HX in methanol (generated *in situ* by addition of $SiMe_3X$) to give the corresponding hydrazine and the dichloro-complexes, $[MoCl_2(NNRPh)(S_2CNR'_2)_2]$. These are non-electrolytes and are analogous to the oxo-complexes $[MoCl_2(O)(S_2CNR'_2)_2]$. Reaction of the bis[hydrazido(2−)]-complexes with 1 equivalent of HX in methanol gives the hydrazido(1−)-derivatives $[Mo(NHNRPh)(NNRPh)(S_2CNR'_2)_2]^+$, isolated as tetraphenylborate salts. Preliminary details have been reported.[9] The reddish brown crystalline complexes are air-stable and have molar conductivities consistent with their being 1:1 electrolytes in dichloromethane solution. Treatment with an excess of triethylamine causes reformation of the parent bis[hydrazido(2−)]-complexes. The synthesis and properties of $[Mo(NHNHCO_2Me)(N_2CO_2Me)(S_2CNMe_2)_2]$ have been reported in detail previously.[10]

The rhenium hydrazido(2−)hydrazido(1−)-complex $[ReCl_2(NHNHCOPh)(NNHCOPh)(PPh_3)_2]$ is isolated as air-stable grey-green crystals by reaction of $[ReCl_2(N_2COPh)(PPh_3)_2]$ with benzoylhydrazine in refluxing methanol. Since $[ReCl_2(N_2COPh)(PPh_3)_2]$ readily undergoes ring-

opening reactions with nucleophiles, the initial product may be $[ReCl_2(H_2NNHCOPh)(N_2COPh)(PPh_3)_2]$, followed by intramolecular hydrogen transfer to give the product.[11]

Structures of Hydrazido(1−)-complexes.—$[Mo(NHNMePh)(NNMePh)(S_2CNMe_2)_2]BPh_4$ (**1**) *and* $[Mo(NHNHCO_2Me)(N_2CO_2Me)(S_2CNMe_2)_2]\cdot 0.5Et_2O$ (**2**). Since both these

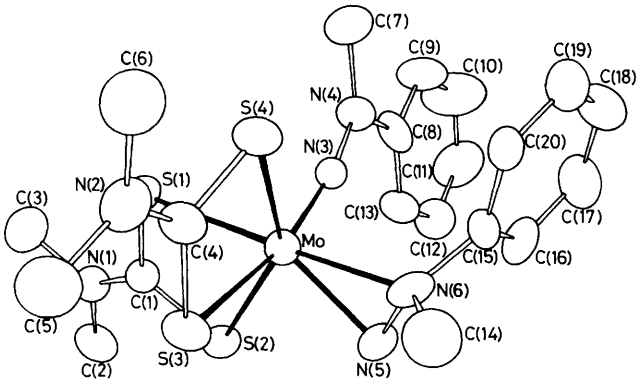

Figure 1. ORTEP view of the structure of $[Mo(NHNMePh)(NNMePh)(S_2CNMe_2)_2]^+$ showing the atom-labelling scheme

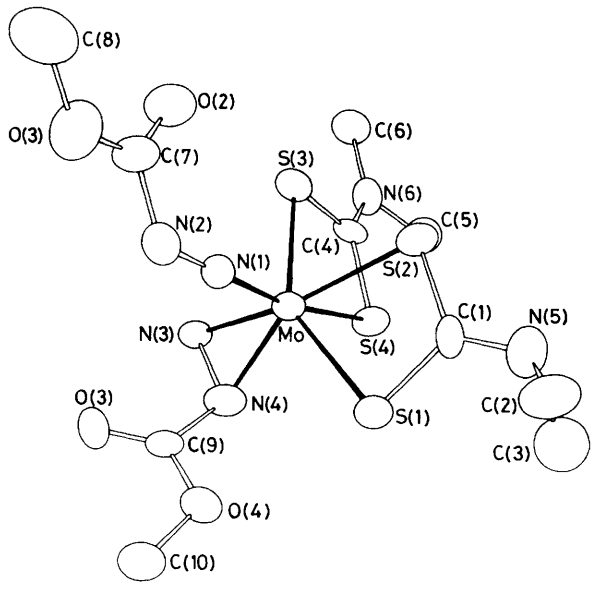

Figure 2. ORTEP view of the structure of $[Mo(NHNHCO_2Me)(NNCO_2Me)(S_2CNMe_2)_2]$ showing the atom-labelling scheme

Table 1. Details of the *X*-ray crystal structure determinations[a]

	$[Mo(NHNMePh)(NNMePh)(S_2CNMe_2)_2]^+$	$[Mo(NHNHCO_2Me)(N_2CO_2Me)(S_2CNMe_2)_2]$	$[ReCl_2(NHNHCOPh)(NNHCOPh)(PPh_3)_2]$
(*i*) Crystal data[b]			
Space group	$P2_1/n$	$C2/c$	$P\bar{1}$
a/Å	16.102(3)	19.963(1)	12.276(2)
b/Å	15.669(5)	18.855(1)	14.147(2)
c/Å	18.752(2)	13.127(1)	15.284(2)
α/°	90.00	90.00	86.33(1)
β/°	112.23(1)	114.41(1)	72.04(1)
γ/°	90.00	90.00	83.10(1)
U/Å^3	4 380.0	4 499.35	2 405.7
Z	4	8	2
D_c/g cm^{-3}	1.36	1.58	1.44
(*ii*) Measurement of intensity data			
Instrument	Nonius CAD4	Nonius CAD4	Nicolet R3m
Scan mode	ω	ω	θ(Crystal)–2θ(counter)
Scan rate/° min^{-1}	Variable between 2 and 30	Variable between 2 and 30	7—30
Scan range/°	$0 < 2\theta < 50$	$0 < 2\theta < 45$	$0 < 2\theta < 45$
Scan length/°	1.2	1.2	$[2\theta(K_{\alpha 1}) - 1.0]$ to $[2\theta(K_{\alpha 2}) + 1.0]$
Background measurement	Stationary crystal, stationary counter at either end of 2θ scan range for 10 s	Stationary crystal, stationary counter at either end of 2θ scan range for 10 s	Stationary crystal, stationary counter at either end of 2θ scan each for time taken for scan
Standard reflections	3 every 100	3 every 100	3 every 197
No. of collected reflections	4 005	2 368	7 205
No. of independent reflections	3 060	1 585	4 995
	$[\lvert I_o\rvert > 2.58\sigma(I_o)]$	$(\lvert F_o\rvert > 6\sigma\lvert F_o\rvert)$	$(\lvert F_o\rvert > 6\sigma\lvert F_o\rvert)$
(*iii*) Reduction of intensity data and structure solution and refinement[c]			
μ/cm^{-1}	5.19	9.56	46.34
Final discrepancy factors R, R'[d]	0.051, 0.065	0.066, 0.08	0.042, 0.043
Goodness of fit[e]	1.92	1.82	1.169

[a] Details common to all three: Mo-K_α radiation (λ = 0.710 69 Å); data corrected for background, attenuators, and Lorentz polarisation in the usual manner; no absorption correction applied; metal atoms located by Patterson synthesis, all other non-hydrogen atoms by Fourier difference synthesis; neutral atom scattering factors used throughout, (D. T. Cromer and J. B. Mann, *Acta Crystallogr., Sect. A*, 1968, **24**, 321); anomalous dispersion applied to all non-hydrogen atoms ('International Tables for *X*-Ray Crystallography,' Kynoch Press, Birmingham, 1962, vol. 3). [b] From a least-squares fitting of the setting angles of 25 reflections. [c] All calculations performed on a Data General Nova 3 computer with 32 K of 16 bit words using local versions of the Nicolet SHELXTL software package, as described by G. M. Sheldrick ('Nicolet SHELXTL Operation Manual,' Nicolet XRD Corporation, Cupertino, CA, 1979). [d] $R = \Sigma[\lvert F_o\rvert - \lvert F_c\rvert/\Sigma F_o]$, $R' = [\Sigma w(\lvert F_o\rvert - \lvert F_c\rvert)^2/\Sigma w\lvert F_o\rvert^2]^{\frac{1}{2}}$, $w = 1/\sigma^2(F_o) + g(F_o)$. [e] $[\Sigma w(\lvert F_o\rvert - \lvert F_c\rvert)^2/N_o - N_v]^{\frac{1}{2}}$ where N_o is the number of observations and N_v is the number of variables.

Table 2. Atomic co-ordinates for $[Mo(NHNMePh)(NNMePh)(S_2CNMe_2)_2]BPh_4$

Atom	*x*	*y*	*z*	Atom	*x*	*y*	*z*
Mo	0.710 80(6)	0.321 13(6)	0.321 13(5)	C(18)	0.873 2(9)	0.250 5(11)	−0.0179
S(1)	0.770 1(2)	0.365 8(2)	0.316 9(2)	C(19)	0.857 4(9)	0.184 1(9)	0.0236
S(2)	0.644 1(2)	0.459 5(2)	0.192 4(2)	C(20)	0.786 7(9)	0.188 1(8)	0.0474
S(3)	0.591 3(2)	0.242 9(2)	0.212 6(2)	B	0.272 7(8)	0.303 7(7)	0.3663
S(4)	0.765 5(2)	0.177 2(2)	0.232 5(2)	C(21)	0.318 0(6)	0.236 2(6)	0.4377
N(1)	0.714 1(6)	0.520 7(6)	0.335 7(5)	C(22)	0.330 4(8)	0.253 6(8)	0.5135
N(2)	0.654 3(6)	0.097 0(6)	0.285 4(5)	C(23)	0.372 8(7)	0.200 1(9)	0.5742
N(3)	0.811 6(6)	0.353 7(6)	0.171 0(5)	C(24)	0.405 9(7)	0.123 3(9)	0.5615
N(4)	0.892 3(6)	0.369 4(7)	0.177 1(5)	C(25)	0.397 6(9)	0.103 3(8)	0.4868
N(5)	0.629 3(6)	0.347 4(6)	0.064 8(5)	C(26)	0.354 4(8)	0.157 8(6)	0.4268
N(6)	0.661 2(6)	0.265 4(5)	0.063 1(5)	C(27)	0.213 6(7)	0.254 1(7)	0.2829
C(1)	0.718 9(7)	0.457 8(7)	0.289 2(6)	C(28)	0.171 5(8)	0.176 0(7)	0.2800
C(2)	0.666 9(8)	0.601 0(7)	0.312 2(8)	C(29)	0.121 1(9)	0.138 4(8)	0.2124
C(3)	0.768 7(10)	0.514 1(9)	0.418 7(8)	C(30)	0.108 8(8)	0.174 2(10)	0.1440
C(4)	0.667 1(8)	0.163 1(7)	0.249 0(7)	C(31)	0.149 1(9)	0.252 3(10)	0.1431
C(5)	0.574 3(9)	0.089 7(9)	0.303 0(9)	C(32)	0.201 2(9)	0.291 1(8)	0.2136
C(6)	0.713 6(11)	0.023 2(8)	0.306 9(8)	C(33)	0.354 8(7)	0.357 7(7)	0.3620
C(7)	0.964 6(8)	0.309 4(9)	0.218 4(7)	C(34)	0.406 6(8)	0.328 1(8)	0.3221
C(8)	0.909 5(8)	0.441 9(8)	0.135 7(7)	C(35)	0.482 0(10)	0.367 7(9)	0.3225
C(9)	0.993 9(9)	0.454 7(9)	0.137 7(10)	C(36)	0.508 3(8)	0.443 6(10)	0.3606
C(10)	1.007 0(13)	0.523 9(15)	0.097 1(14)	C(37)	0.460 8(8)	0.477 6(8)	0.4001
C(11)	0.938 1(13)	0.578 5(12)	0.057 0(10)	C(38)	0.386 3(7)	0.435 0(7)	0.4016
C(12)	0.854 3(10)	0.562 0(8)	0.055 3(8)	C(39)	0.192 9(7)	0.363 2(7)	0.3797
C(13)	0.839 1(8)	0.495 9(8)	0.096 1(7)	C(40)	0.170 5(7)	0.444 3(7)	0.3498
C(14)	0.593 2(9)	0.193 6(9)	0.036 1(9)	C(41)	0.097 5(9)	0.486 9(8)	0.3544
C(15)	0.729 9(7)	0.259 4(7)	0.029 6(6)	C(42)	0.045 1(9)	0.453 2(9)	0.3892
C(16)	0.747 1(10)	0.326 1(8)	−0.011 1(7)	C(43)	0.063 3(8)	0.371 6(9)	0.4195
C(17)	0.818 5(11)	0.318 5(10)	−0.035 4(8)	C(44)	0.136 3(7)	0.328 1(8)	0.4141

Table 3. Selected bond lengths (Å) and angles (°) for $[Mo(NHNMePh)(NNMePh)(S_2CNMe_2)_2]BPh_4$

Mo–S(1)	2.512(3)	N(3)–N(4)	1.28(1)
Mo–S(2)	2.480(3)	N(1)–C(1)	1.30(1)
Mo–S(3)	2.564(4)	N(1)–C(2)	1.45(1)
Mo–S(4)	2.496(3)	N(1)–C(3)	1.47(2)
Mo–N(3)	1.75(1)	N(2)–C(4)	1.30(2)
Mo–N(5)	2.070(8)	N(2)–C(5)	1.45(2)
Mo–N(6)	2.176(9)	N(2)–C(6)	1.46(2)
N(5)–N(6)	1.39(2)		
S(1)–Mo–S(2)	67.1(1)	S(3)–Mo–S(4)	69.3(1)
S(1)–Mo–S(3)	84.1(1)	S(3)–Mo–N(3)	164.3(3)
S(1)–Mo–S(4)	83.7(1)	S(3)–Mo–N(5)	96.3(3)
S(1)–Mo–N(3)	89.8(1)	S(3)–Mo–N(6)	91.7(3)
S(1)–Mo–N(5)	148.5(3)	S(4)–Mo–N(3)	95.8(3)
S(1)–Mo–N(6)	172.5(2)	S(4)–Mo–N(5)	126.1(4)
S(2)–Mo–S(3)	89.6(1)	S(4)–Mo–N(3)	87.1(3)
S(2)–Mo–S(4)	147.7(1)	N(3)–Mo–N(5)	96.5(4)
S(2)–Mo–N(3)	101.8(3)	N(3)–Mo–N(6)	92.7(4)
S(2)–Mo–N(5)	78.8(2)	N(5)–Mo–N(6)	38.1(4)
S(2)–Mo–N(6)	116.6(3)	Mo–N(5)–N(6)	75.1(6)
Mo–N(6)–N(5)	66.8(3)		

Figure 3. Bond lengths (Å) and angles (°) for NN′-bonded hydrazido(1−)-ligands in complexes (**1**) and (**2**)

complexes contain NN′-bonded hydrazido(1−)-ligands these are considered together. The crystal data are summarised in Table 1. An ORTEP view of the structure of $[Mo(NHNMePh)(NNMePh)(S_2CNMe_2)_2]BPh_4$ is shown in Figure 1 together with the atom-labelling scheme. Table 2 gives atomic co-ordinates and Table 3 selected bond lengths and angles. Atomic co-ordinates for $[Mo(NHNHCO_2Me)(N_2CO_2Me)(S_2CNMe_2)_2]\cdot 0.5Et_2O$ are given in Table 4, selected bond lengths and angles in Table 5, and Figure 2 gives an ORTEP view of the structure of this complex.

A comparison of the bond lengths and angles within the hydrazido(1−)-ligands is given in Figure 3. Despite the variations in substituents the values are extremely similar. The Mo–N bond lengths suggest that there is little multiple bonding between nitrogen and molybdenum. The N–N bond length is close to that found in hydrazine itself and corresponds to a single bond. In general the dimensions of the hydrazido(1−)-ligand are very similar to those found in $[TiCl_2(\eta^5\text{-}C_5H_5)(H_2NNPh)]$[12] suggesting that they are relatively insensitive to the metal ion and its ligand environment. In complex (**1**) the Mo–N(5)–N(6) plane and the N(5)–N(6)–C(14)–C(15) system are approximately planar. This suggests approximate sp^2 hybridisation for N(6) with the remaining *p* orbital being used to bond to the metal. The hydrogen on N(5) was not located in the structure, preventing any consideration of the hybridisation involved.

In $[Mo(NHNMePh)(NNMePh)(S_2CNMe_2)_2]^+$ the unreacted hydrazido(2−)-ligand occupies an axial site and has similar geometry and dimensions to the hydrazido-ligands in the parent bis[hydrazido(2−)]-complex,[8] and in other hydrazido(2−)-complexes. The methoxycarbonyldiazenido-ligand in $[Mo(NHNHCO_2Me)(N_2CO_2Me)(S_2CNMe_2)_2]$ (**2**) occupies an analogous axial site and the bond lengths and angles are similar to those found in other diazenido-complexes. It is perhaps remarkable that the MeOCONHNH ligand should be NN′-bonded when there is a possibility of forming a stable

Table 4. Atomic co-ordinates for $[Mo(NHNHCO_2Me)(N_2CO_2Me)(S_2CNMe_2)_2]\cdot 0.5Et_2O$

Atom	*x*	*y*	*z*	Atom	*x*	*y*	*z*
Mo	0.210 9(1)	0.385 9(1)	0.086 7(1)	O(4)	0.249 8(7)	0.378 3(6)	0.381 8(10)
S(1)	0.171 7(1)	0.482 6(1)	0.179 9(1)	C(1)	0.115 3(8)	0.516 6(7)	0.050 2(13)
S(2)	0.117 2(2)	0.465 1(2)	−0.056 5(2)	C(2)	0.026 6(11)	0.598 1(10)	0.082 16(16)
S(3)	0.228 1(2)	0.350 4(2)	−0.083 1(2)	C(3)	0.077 6(11)	0.619 3(10)	0.129 6(16)
S(4)	0.311 4(2)	0.463 6(2)	0.064 3(2)	C(4)	0.294 5(9)	0.413 5(7)	−0.054 6(11)
N(1)	0.146 3(7)	0.321 4(6)	0.077 4(10)	C(5)	0.314 3(10)	0.380 0(10)	−0.218 8(13)
N(2)	0.098 1(7)	0.273 1(6)	0.071 3(10)	C(6)	0.383 9(9)	0.482 9(9)	−0.100 3(5)
N(3)	0.299 4(6)	0.315 2(6)	0.174 6(9)	C(7)	0.072 6(7)	0.233 1(9)	−0.026 6(14)
N(4)	0.290 8(7)	0.364 0(7)	0.248 2(11)	C(8)	0.012 9(14)	0.143 7(13)	−0.114 6(19)
N(5)	0.075 3(7)	0.572 7(7)	0.035 2(12)	C(9)	0.272 9(9)	0.329 0(9)	0.329 4(10)
N(6)	0.329 7(7)	0.425 3(7)	−0.121 2(10)	C(10)	0.228 3(12)	0.350 5(10)	0.466 2(16)
O(1)	0.089 0(7)	0.237 5(7)	−0.104 0(10)	O(5)	0	0.099(2)	0.250 0(0)
O(2)	0.023 1(7)	0.188 6(7)	−0.022 2(13)	C(11)	0.043 2(16)	0.120 6(17)	0.332(3)
O(3)	0.275 9(8)	0.266 7(6)	0.343 6(10)	C(12)	0.071(2)	0.191(2)	0.359(4)

Table 5. Selected bond lengths (Å) and angles (°) for $[Mo(NHNHCO_2Me)(N_2CO_2Me)(S_2CNMe_2)_2]\cdot 0.5Et_2O$

Mo–S(1)	2.495(5)	N(2)–C(7)	1.39(2)
Mo–S(2)	2.521(4)	N(4)–C(9)	1.42(2)
Mo–S(3)	2.483(5)	N(5)–C(1)	1.29(2)
Mo–S(4)	2.597(5)	N(5)–C(2)	1.44(2)
Mo–N(1)	1.74(1)	N(5)–C(3)	1.50(2)
Mo–N(3)	2.13(1)	N(6)–C(4)	1.35(2)
Mo–N(4)	2.10(1)	N(6)–C(4)	1.46(2)
N(1)–N(2)	1.30(2)	N(6)–C(5)	1.48(2)
N(3)–N(4)	1.40(2)		
S(1)–Mo–S(2)	69.3(1)	Mo–S(1)–C(1)	89.8(11)
S(1)–Mo–S(3)	145.6(1)	Mo–S(2)–C(1)	89.2(10)
S(1)–Mo–S(4)	93.3(1)	Mo–S(3)–C(4)	89.9(12)
S(1)–Mo–N(1)	99.9(5)	Mo–S(4)–C(4)	85.6(12)
S(1)–Mo–N(3)	123.3(5)	Mo–N(1)–N(2)	179.6(15)
S(1)–Mo–N(4)	84.8(5)	N(1)–N(2)–C(7)	114.5(16)
S(2)–Mo–S(3)	80.0(1)	Mo–N(4)–N(3)	72.0(12)
S(2)–Mo–S(5)	87.2(1)	S(3)–Mo–N(4)	121.6(6)
S(2)–Mo–N(1)	93.5(5)	S(4)–Mo–N(1)	166.2(5)
S(2)–Mo–N(3)	165.3(5)	S(4)–Mo–N(3)	84.7(6)
S(2)–Mo–N(4)	152.7(5)	S(4)–Mo–N(4)	85.7(5)
S(3)–Mo–S(4)	69.5(1)	N(1)–Mo–N(3)	91.5(7)
S(3)–Mo–N(1)	97.0(5)	N(1)–Mo–N(4)	99.5(7)
S(3)–Mo–N(3)	85.8(5)	N(3)–Mo–N(4)	38.5(7)

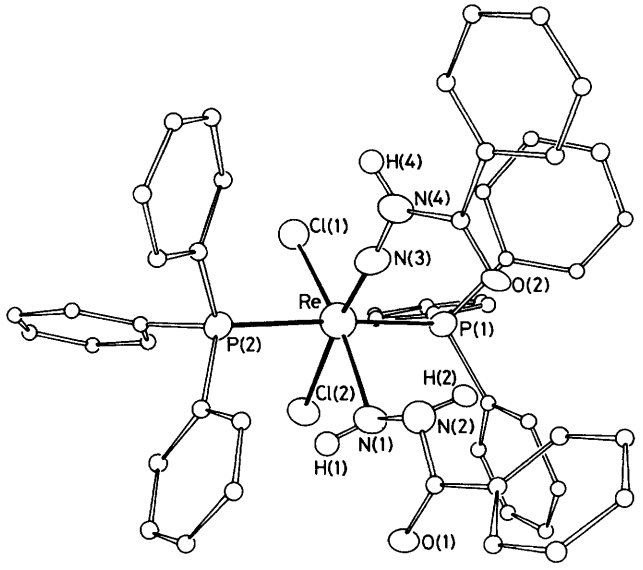

Figure 4. ORTEP view of the structure of $[ReCl_2(NHNHCOPh)(NNHCOPh)(PPh_3)_2]$ showing the atom-labelling scheme

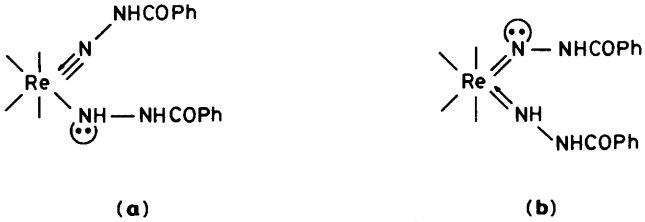

Figure 5. Possible structures for $[ReCl_2(NHNHCOPh)(NNHCOPh)(PPh_3)_2]$

five-membered chelate-ring system Mo–NH–NH–CO–OMe utilising the carbonyl oxygen.

$[ReCl_2(NHNHCOPh)(NNHCOPh)(PPh_3)_2]$ (**3**). The crystal data for $[ReCl_2(NHNHCOPh)(NNHCOPh)(PPh_3)_2]$ (**3**) are summarised in Table 1. An ORTEP view of the molecule is presented in Figure 4 together with the atom-labelling scheme. Table 6 gives atomic co-ordinates and Table 7 bond lengths and angles.

Two peaks appearing in the final electron-density map adjacent to N(1) and N(2) were assigned to hydrogens, confirming the presence of a hydrazido(1−)-ligand. Similarly the hydrogen attached to N(4) was located, confirming that a hydrazido(2−)-ligand is also present. Simple valence-electron-counting arguments predict two possible structures (**a**) and (**b**) (Figure 5) containing hydrazido(1−)- and hydrazido(2−)-ligand systems. The *X*-ray analysis unequivocally confirms that structure (**a**) is preferred with a terminal N-bonded hydrazido(1−)-ligand functioning formally as a one-electron ligand. In this instance it appears that steric and electronic effects combine to prevent the hydrazido(1−)-ligand bonding in a NN′-fashion to the metal.

The bond lengths within the hydrazido(2−)-ligand NNHCOPh [M–N 1.728(7), N–N 1.27(1) Å] are well within the range found for other linear, formally four-electron-donor hydrazido(2−)-ligands. The only other structurally characterised example of an N-bonded hydrazido(1−)-complex is $[Mo\{HB(3,5Me_2\text{-}pz)_3\}(NO)(NHNMe_2)]$ ($3,5Me_2$-pz = 3,5-dimethylpyrazolyl).[13] Comparison of the bond lengths within the Re and Mo structures (Table 8) suggests a significantly larger contribution of canonical form (**c**) relative to (**d**) (Figure 6) for the molybdenum complex. This is revealed by the smaller Mo–N–N angle and shorter metal–nitrogen distance.

It is interesting to compare the structure of $[ReCl_2(NHNH-$

Table 6. Atomic co-ordinates for $[ReCl_2(NHNHCOPh)(NNHCOPh)(PPh_3)_2]$

Atom	*x*	*y*	*z*	Atom	*x*	*y*	*z*
Re	2 118(1)	1 460(1)	2 043(1)	C(43)	3 493(11)	−506(8)	5 112(8)
P(2)	849(2)	2 634(2)	1 441(2)	C(44)	2 332(9)	−521(8)	5 580(8)
P(1)	3 468(2)	193(2)	2 456(2)	C(45)	1 544(9)	−389(7)	5 100(7)
Cl(1)	824(2)	271(2)	2 136(2)	C(46)	1 887(8)	−188(7)	4 159(6)
Cl(2)	3 145(2)	1 221(2)	427(2)	C(51)	3 735(8)	−969(6)	1 909(6)
N(1)	3 479(6)	2 435(5)	1 708(5)	C(52)	3 538(9)	−1 077(8)	1 096(7)
N(2)	3 454(6)	3 132(5)	2 361(5)	C(53)	3 844(10)	−1 946(8)	646(8)
N(3)	1 473(6)	1 787(5)	3 173(5)	C(54)	4 335(10)	−2 692(8)	1 013(8)
N(4)	946(6)	1 955(5)	4 017(4)	C(55)	4 561(12)	−2 620(11)	1 810(10)
O(1)	1 379(7)	3 508(5)	3 815(5)	C(56)	4 256(10)	−1 736(9)	2 282(9)
O(2)	5 164(6)	3 503(5)	1 431(5)	C(61)	1 615(8)	3 600(6)	800(6)
C(10)	4 342(8)	3 671(7)	2 127(7)	C(62)	1 941(8)	4 285(7)	1 274(7)
C(11)	4 260(8)	4 469(7)	2 747(6)	C(63)	2 668(9)	4 973(8)	799(7)
C(12)	3 235(9)	4 953(7)	3 207(7)	C(64)	3 040(10)	4 964(9)	−141(8)
C(13)	3 169(10)	5 715(8)	3 764(7)	C(65)	2 737(11)	4 316(9)	−620(9)
C(14)	4 206(10)	5 967(8)	3 845(8)	C(66)	2 011(9)	3 613(8)	−157(7)
C(15)	5 233(10)	5 464(8)	3 390(7)	C(71)	−367(7)	3 200(6)	2 332(6)
C(16)	5 277(9)	4 724(7)	2 830(7)	C(72)	−965(7)	2 634(7)	3 047(6)
C(20)	923(8)	2 860(6)	4 318(6)	C(73)	−1 906(9)	3 036(8)	3 740(8)
C(21)	275(8)	2 982(7)	5 294(6)	C(74)	−2 339(10)	3 987(8)	3 705(8)
C(22)	230(9)	3 851(7)	5 695(7)	C(75)	−1 667(10)	4 564(8)	2 995(7)
C(23)	−345(10)	3 959(9)	6 625(8)	C(76)	−732(8)	4 172(7)	2 302(7)
C(24)	−885(11)	3 243(9)	7 141(9)	C(81)	140(7)	2 270(6)	633(6)
C(25)	−864(11)	2 394(9)	6 761(9)	C(82)	463(8)	1 419(7)	200(6)
C(26)	−254(9)	2 254(8)	5 840(7)	C(83)	−49(8)	1 195(7)	−433(6)
C(31)	4 915(7)	549(6)	2 222(6)	C(84)	−902(9)	1 802(8)	−635(7)
C(32)	5 086(9)	1 269(7)	2 754(7)	C(85)	−1 227(11)	2 651(9)	−197(8)
C(33)	6 169(9)	1 586(8)	2 564(7)	C(86)	−715(10)	2 883(8)	442(7)
C(34)	7 050(11)	1 196(8)	1 871(8)	C(1)	6 072(18)	7 012(15)	5 169(15)
C(35)	6 900(11)	516(9)	1 319(8)	C(2)	6 623(19)	7 653(15)	4 473(15)
C(36)	5 818(9)	194(8)	1 512(7)	O(3)	6 665(16)	7 431(13)	3 659(13)
C(41)	3 056(7)	−123(6)	3 683(6)	C(4)	7 280(26)	8 151(21)	3 058(19)
C(42)	3 833(9)	−294(7)	4 181(7)	C(5)	7 631(23)	7 711(19)	3 238(18)

Table 7. Selected bond lengths (Å) and angles (°) for $[ReCl_2(NHNHCOPh)(NNHCOPh)(PPh_3)_2]$

Re–P(2)	2.470(2)	Re–P(1)	2.479(2)
Re–Cl(1)	2.416(3)	Re–Cl(2)	2.427(2)
Re–N(1)	2.212(8)	Re–N(3)	1.730(7)
N(1)–N(2)	1.438(11)	N(3)–N(4)	1.275(9)
N(2)–C(10)	1.350(13)	N(4)–C(20)	1.383(12)
C(20)–O(1)	1.229(11)	C(10)–O(2)	1.233(10)
P(2)–Re–P(1)	172.9(1)	P(2)–Re–Cl(1)	89.61(1)
P(1)–Re–Cl(1)	89.5(1)	P(2)–Re–Cl(2)	83.8(1)
P(1)–Re–Cl(2)	89.5(1)	Cl(1)–Re–Cl(2)	94.4(1)
P(2)–Re–N(1)	91.3(2)	P(1)–Re–N(1)	89.3(2)
Cl(1)–Re–N(1)	169.4(2)	Cl(2)–Re–N(1)	75.2(2)
P(2)–Re–N(3)	93.8(2)	P(1)–Re–N(3)	93.2(2)
Cl(1)–Re–N(3)	93.7(2)	Cl(2)–Re–N(3)	175.5(2)
N(1)–Re–N(3)	96.8(3)		

COPh)(NNHCOPh)$(PPh_3)_2$] with that of $[ReCl_2(NNHPh)(NNPh)(PPh_3)_2]$.[14] For the latter complex, electron-counting arguments indicate that the hydrazido(2−) (NNHPh) and

Figure 6. Resonance forms for the hydrazido(1−)-ligand $NHNR_2$

diazenido (N_2Ph) ligands cannot both be linear as this would give the metal 20 valence electrons. In this situation the hydrazido(2−)-ligand bends in preference to the diazenido-ligand. Comparison of the two structures therefore suggests that the relative ease of bending at the nitrogen adjacent to the metal is in the sequence hydrazido(1−) > hydrazido(2−) > diazenido(1−) (all N-bonded).

Kinetics of the Reaction of Acids with $[Mo(NNRPh)_2(S_2CNR'_2)_2]$.—Previous attempts to investigate the ammonia (or hydrazine)-forming reactions of hydrazido(2−)-complexes[15] were complicated by the concomitant decomposition

Table 8. Comparison of the structures of hydrazido-complexes

	Hydrazido(1−)-ligand			Hydrazido(2−)-ligand			
Complex	M–N/Å	N–N/Å	M–N–N/°	M–N/Å	N–N/Å	M–N–N/°	Ref.
$[Mo\{HB(3,5Me_2\text{-}pz)_3\}(NO)(NHNMe_2)]$	1.98(2)	1.34(3)	140.3(15)				13
$[ReCl_2(NNHPh)(NNPh)(PPh_3)_2]$				1.922(11)	1.287(12)	131.2(10)	14
$[ReCl_2(NHNHCOPh)(NNHCOPh)(PPh_3)_2]$	2.212(8)	1.44(1)	116.1(7)	1.730(7)	1.275(9)	174.7(7)	This work

Table 9. Analytical and spectroscopic characterisation of hydrazido-complexes

Complex	Structure	Analysis (%)[a] C	H	N	^{1}H N.m.r. (p.p.m.)[b] Hydrazido	Dithiocarbamate
$[Mo(NNMePh)_2(S_2CNMe_2)_2]$	(A)	42.2 (42.2)	4.8 (4.8)	14.5 (14.5)	4.02(s, 6, NN*Me*Ph) 6.80—7.43 (m, 10, NNMe*Ph*)	3.32 (s, 12, Me)
$[Mo(NNPh_2)_2(S_2CNEt_2)_2]$	(A)	53.8 (54.0)	5.0 (5.2)	11.0 (11.1)	6.96—7.40 (m, 20, Ph_2)	1.26 (br, 12, Me) 3.75 (br, 8, CH_2)
$[Mo(NHNMePh)(NNMePh)(S_2CNMe_2)_2]BPh_4$	(D)	58.7 (58.9)	5.3 (5.5)	9.6 (9.4)	*c*	
$[MoCl_2(NNMePh)(S_2CNMe_2)_2]$	(H)	29.6 (29.6)	3.9 (3.9)	10.4 (10.6)	3.95 (s 3, Me) 7.0—7.6 (m, 5, Ph)	3.27 (d, 12, Me)
$[MoCl_2(NNPh_2)(S_2CNEt_2)_2]$	(H)	40.5 (40.9)	5.1 (4.7)	9.1 (8.7)	6.93—7.36 (m, 10 Ph)	1.17 [t, 6, *J*(HH) 6.9, Me] 1.19 [t, 6, *J*(HH) 4.8, Me] 3.43—3.88 (m, 8, CH_2)
$[ReCl_2(NHNHCOPh)(NNHCOPh)(PPh_3)_2]\cdot 0.5Et_2O$		53.3 (53.0)	4.5 (4.0)	5.1 (5.2)		

[a] Calculated values in parentheses. [b] s = Singlet, d = doublet, t = triplet, m = multiplet, br = broad. Multiplicities, relative intensities, *J* values (Hz), and assignments are given in parentheses. [c] Poor stability precluded recording of ^{1}H n.m.r. spectrum.

of solvent tetrahydrofuran (thf), equation (1).[16] However, the

$$\overbrace{O(CH_2)_3CH_2} + HX \longrightarrow HO(CH_2)_4X \quad (1)$$

rate of reaction (2) is much faster than that of reaction (1), and

$$cis\text{-}[Mo(NNRPh)_2(S_2CNR'_2)_2] + 3HCl \longrightarrow [MoCl_2(NNRPh)(S_2CNR'_2)_2] + RPhNNH_3{}^+Cl^- \quad (2)$$

so complications attributable to the latter are avoided.

The complexes *cis*-$[Mo(NNRPh)_2(S_2CNR'_2)_2]$ (**A**),[8] $[MoCl_2(NNRPh)(S_2CNR'_2)_2]$ (**G**),[8] and $[Mo(NHNMePh)(NNMePh)(S_2CNMe_2)_2]BPh_4$ (**D**)[9] were prepared by the literature methods or as below, and characterised analytically and spectroscopically as shown in Table 9. The structures of (**A**; R = Ph, R′ = Me)[8] and (**D**; R = R′ = Me)[9] have been determined by *X*-ray crystallography. The nature of the substituent R′ has little effect on the reactions described herein as demonstrated by the similar results for the kinetics of hydrazido-formation from (**A**; R = Ph, R′ = Et) and from (**A**; R = Ph, R′ = Me).

The stoicheiometry of the reaction between complexes (**A**) and HCl was determined spectrophotometrically (Figure 7), and for R = R′ = Me is associated with an isosbestic point at λ = 462 nm, and for R = Ph, R′ = Et, with an isosbestic point at 425 nm. The observed stoicheiometry (2) is a consequence of the relatively strong basicity of the liberated hydrazine, consuming 1 mol equivalent of acid.

It is most convenient to present the kinetic results of reaction (2) in separate sections corresponding to the various substrates (**A**), with different R and R′ groups, and the studies on the reactions of (**D**) with acids or bases under a subsequent common heading. The letters used correspond to those in the Scheme.

Protonation of cis-$[Mo(NNMePh)_2(S_2CNMe_2)_2]$. The reaction of complex (**A**; R = R′ = Me) with HCl occurs in two stages: an initial rapid reaction which is complete within the dead-time of the stopped-flow apparatus ($k_{obs.} > 300$ s^{-1}), followed by a relatively slow reaction to yield the corresponding product (**G**) and hydrazine. The absorbance–time curves are biphasic, comprising the rate constants, $k_{obs.}'' = (2.5 \pm 0.5) \times 10^{-3}$ and $k_{obs.}' = (1.6 \pm 0.2) \times 10^{-2}$ s^{-1}. The slower reaction corresponds to 22% of the total absorbance change, independent of the acid concentration.

Under all conditions the slow phases exhibit a first-order dependence on the concentration of the complex, but are independent of both the concentration and nature of the acid (Table 10).

The initial absorbance is dependent upon the concentration of HCl (Table 11). Simple analysis of these data shows that more than one proton is involved in this phase. If the concentration of acid is in a large excess over the concentration of complex, and 'tight' ion pairs are formed between chloride ions and species (**B**) and (**C**), then, as described in equations (3) and (4), the relationship (5) holds. The subscripts e and o refer to

$$K_1^R K_2^R = \frac{[C]_e}{[A]_e[HCl]^2} = \frac{([A]_o - [A]_e - [B]_e)}{[A]_e[HCl]^2} \quad (3)$$

$$K_1^R + K_1^R K_2^R[HCl] = \left(\frac{[A]_o}{[A]_e} - 1\right)\frac{1}{[HCl]} \quad (4)$$

$$K_1^R + K_1^R K_2^R[HCl] = \frac{([B]_e + [C]_e)}{[A]_e[HCl]} \quad (5)$$

the equilibrium and total concentrations respectively. Using the values of $\varepsilon_A = 1.42 \times 10^4$ dm^3 mol^{-1} cm^{-1} (**A**; R = R′ = Me), and $\varepsilon_B + \varepsilon_C = 1.02 \times 10^4$ dm^3 mol^{-1} cm^{-1} at λ = 370 nm, the right-hand term of equation (5) was determined at each concentration of acid, and plotted against the corresponding acid concentrations as shown in Figure 8. The derived values ($K_1^{Me} = 120 \pm 5$, $K_2^{Me} = 140 \pm 20$ dm^3 mol^{-1}) show that despite the increased charge on species (**B**) the equilibrium constants for the two protonations are essentially identical.

The spectrum of the equilibrium mixture of complexes (**B**) and (**C**) was measured at [HCl] = 25.0 mmol dm^{-3} and is shown in Figure 9. An identical spectrum is observed using [HBr] = 0.5 mmol dm^{-3}, indicating that these species do not contain halide.

Protonation of cis-$[Mo(NNPh_2)_2(S_2CNEt_2)_2]$. The reaction between complex (**A**; R = Ph, R′ = Et) and an excess of HCl occurs in three distinct phases: an initial rapid reaction which is complete within the dead-time of the stopped-flow apparatus ($k_{obs.} > 300$ s^{-1}), followed by a biphasic reaction to yield the product (**G**) and the corresponding hydrazine. Thus the behaviour observed with this substrate is analogous to that shown by (**A**; R = R′ = Me). Both phases occur at a rate exhibiting a first-order dependence on the concentration of

Table 10. Kinetics of the reactions between HX (X = Cl or Br) and *cis*-$[Mo(NNRPh)_2(S_2CNR'_2)_2]$

R	X	[HX] mmol dm^{-3}	[NEt_4Cl] mmol dm^{-3}	$k_{obs.}'$/s^{-1}	$k_{obs.}''$/s^{-1}
Me[a]	Cl	1.00		1.3×10^{-2}	3.1×10^{-3}
		1.00[b]		1.7×10^{-2}	3.0×10^{-3}
		2.00		1.5×10^{-2}	2.6×10^{-3}
		5.00		1.6×10^{-2}	2.4×10^{-3}
		10.00		1.7×10^{-2}	2.1×10^{-3}
		10.00[b]		1.5×10^{-2}	2.0×10^{-3}
		20.00		1.5×10^{-2}	2.2×10^{-3}
		50.00		1.6×10^{-2}	2.5×10^{-3}
		100.00		1.6×10^{-2}	2.1×10^{-3}
		100.00[b]		1.5×10^{-2}	2.4×10^{-3}
		100.00	0.10	1.8×10^{-2}	2.4×10^{-3}
			0.50	1.6×10^{-2}	2.1×10^{-3}
			1.00	1.7×10^{-2}	2.6×10^{-3}
			2.00	1.6×10^{-2}	2.5×10^{-3}
			5.00	1.8×10^{-2}	2.1×10^{-3}
			10.00	1.8×10^{-2}	2.4×10^{-3}
	Br	0.50		1.8×10^{-2}	2.5×10^{-3}
		1.00		1.7×10^{-2}	2.7×10^{-3}
		2.00		1.8×10^{-2}	2.5×10^{-3}
		4.00		1.9×10^{-2}	2.1×10^{-3}
		10.00		2.0×10^{-2}	2.2×10^{-3}
Ph[a]	Cl	1.25		0.70	1.2×10^{-2}
		2.50		0.55	1.5×10^{-2}
		2.50[b]		0.52	1.5×10^{-2}
		5.00		0.55	1.8×10^{-2}
		5.00[b]		0.55	1.8×10^{-2}
		10.00		0.50	1.9×10^{-2}
		10.00[b]		0.53	1.8×10^{-2}
		15.00		0.46	1.4×10^{-2}
		20.00		0.46	1.5×10^{-2}
		30.00		0.46	1.2×10^{-2}
		40.00		0.46	1.2×10^{-2}
		40.00[b]		0.50	1.2×10^{-2}
		50.00		0.48	1.3×10^{-2}
		20.00	0.10	0.48	1.5×10^{-2}
			0.50	0.55	1.3×10^{-2}
			1.00	0.52	1.2×10^{-2}
			2.00	0.57	1.3×10^{-2}
			5.00	0.58	1.3×10^{-2}
			10.00	0.56	1.5×10^{-2}
	Br	0.50		0.60	1.4×10^{-2}
		1.00		0.55	1.2×10^{-2}
		2.00		0.51	1.3×10^{-2}
		4.00		0.55	1.3×10^{-2}
Ph[c]	Cl	1.00		0.45	1.4×10^{-2}
		2.50		0.42	1.7×10^{-2}
		5.00		0.42	1.8×10^{-2}
		25.00		0.40	1.8×10^{-2}
		50.00		0.40	2.0×10^{-2}
Me[d]	Cl	0.50		3.5×10^{-3}[e]	
		0.50[b]		3.0×10^{-3}	
		1.00		3.1×10^{-3}	
		1.00[b]		3.1×10^{-3}	
		2.00		3.3×10^{-3}	
		4.00		3.0×10^{-3}	
		4.00[b]		3.5×10^{-3}	
		10.00		2.9×10^{-3}	
		10.00	0.10	2.7×10^{-3}	
			0.50	2.8×10^{-3}	
			1.00	3.1×10^{-3}	
			10.00	2.7×10^{-3}	

[a] [Mo] = 5.0×10^{-5} mol dm^{-3}. [b] Studies using ^{2}HCl. [c] Studies using $[Mo(NNPh_2)_2(S_2CNMe_2)_2]$. [d] Studies on (**D**; R = R′ = Me). [e] Exponential absorbance–time curve.

complex, but independent of the concentration and nature of the acid [$k_{obs.}' = 0.51 \pm 0.05$, $k_{obs.}'' = (1.5 \pm 0.3) \times 10^{-2}$ s^{-1}]. The kinetic data are shown in Table 10.

Table 11. Influence of the concentration of HCl on the initial absorbance in the reactions with *cis*-$[Mo(NNRPh)_2(S_2CNR'_2)_2]$ (R = R′ = Me or R = Ph, R′ = Et) at 25.0 °C and I = 0.1 mol dm^{-3}($[NBu^n_4]BF_4$)

R	λ/nm	[HCl]/ mmol dm^{-3}	Absorbance
Me*	370	0.00	0.710
		0.25	0.708
		0.50	0.697
		1.00	0.687
		2.00	0.660
		3.00	0.619
		5.00	0.590
		10.00	0.560
		25.00	0.530
		50.00	0.520
		100.00	0.510
Ph*	500	0.00	0.008
		1.00	0.021
		2.50	0.038
		5.00	0.053
		10.00	0.084
		25.00	0.113
		50.00	0.161
		100.00	0.189
		200.00	0.200

* [Mo] = 5.0×10^{-5} mol dm^{-3}.

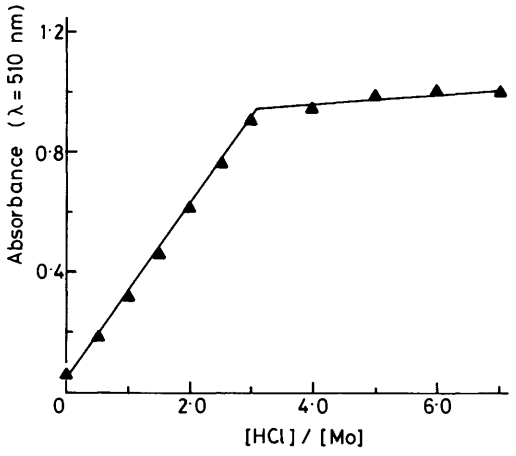

Figure 7. Typical spectrophotometric titration to determine the stoicheiometry of the reaction between *cis*-$[Mo(NNPh_2)_2(S_2CNEt_2)_2]$ and HCl in tetrahydrofuran. [Mo] = 1.06×10^{-4} mol dm^{-3}

Analogous to the behaviour observed with complex (**A**; R = R′ = Me), the magnitude of the initial absorbance depends on the concentration of HCl, as shown in Table 11. Using the values of $\varepsilon_A = 3.2 \times 10^2$ (**A**; R = Ph, R′ = Et) and $\varepsilon_B = 8.0 \times 10^3$ dm^3 mol^{-1} cm^{-1}, (**B**; R = Ph, R′ = Et) at λ = 500 nm, and analysing the data using equation (5) (as shown in Figure 8) shows that only one proton is involved in this initial equilibrium ($K_1^{Ph} = 75 \pm 3$ dm^3 mol^{-1}), whereas for (**A**; R = R′ = Me) more than one proton is involved.

The spectra of complex (**B**) and of the intermediate formed subsequently were measured at [HCl] = 100.0 mmol dm^{-3}, and are shown in Figure 10.

Reactivity of $[Mo(NHNMePh)(NNMePh)(S_2CNMe_2)_2]^+$. The complex (**D**; R = R′ = Me) reacts with an excess of HCl to give (**G**) and the corresponding hydrazine, at a rate independent

Table 12. Kinetics of the reactions between $[Mo(NHNMePh)(NNMePh)(S_2CNMe_2)_2]^+$ (**D**) and base (Cl^-, NEt_2H, NEt_3, or NBu^n_3) in tetrahydrofuran at 25.0 °C, λ = 355 nm, and I = 0.1 mol dm^{-3} ($NBu^n_4BF_4$)[a]

Base	[Base] mmol dm^{-3}	[NEt_3H^+] mmol dm^{-3}	$k_{obs.}/s^{-1}$
NEt_3	0.05		10.3[b]
	0.10		19.5[b]
	0.20		27.0
	0.20[c]		30.0
	0.40		53.0
	0.40[c]		54.1
	0.60		72.4
	0.70		90.8
	0.80		92.4
	1.0		115.0
	1.0[c]		118.4
	1.5		140.2
	2.0		175.8
	2.0[c]		170.8
	0.25	0.50	38.2
		1.00	37.6
		2.50	39.1
		5.00	38.5
		10.00	39.8

Base	[Base]/ mmol dm^{-3}	$k_{obs.}/s^{-1}$
NBu^n_3	0.05	20.1
	0.10	38.9
	0.20	71.0
	0.40	132.0
	0.60	144.3
	0.80	152.1
	1.00	173.0
	1.50	236.1
	2.00	260.7
NEt_2H	0.10	250
	0.20	270
	0.40	270
	0.80	270
	1.50	270
	3.00	250
$[NBu_4]Cl$	0.10	250
	0.25	270
	0.50	270
	1.00	260
	2.00	260

[a] [Mo] = 5×10^{-5} mol dm^{-3}. [b] Non-exponential absorbance–time traces, rate constant estimated by fit to initial slope. [c] Studies with $[Mo(N^2HNMePh)(NNMePh)(S_2CNMe_2)_2]BPh_4$.

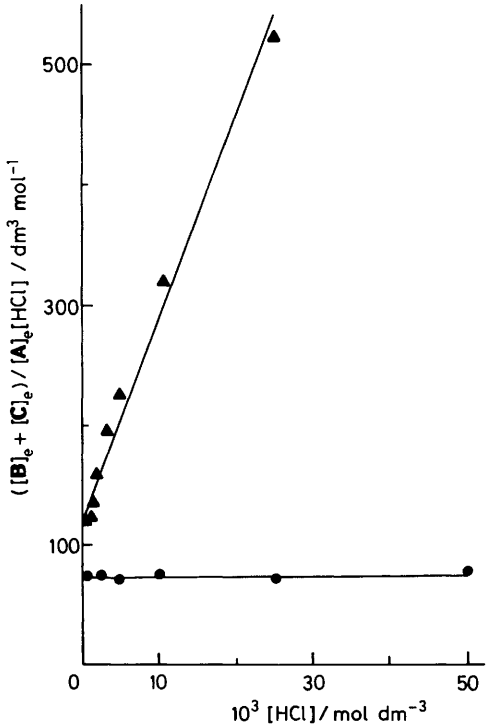

Figure 8. Dependence of the value of $([B]_e + [C]_e)/[A]_e[HCl]$ on the concentration of HCl for the reactions of complexes (**A**; R = R′ = Me) (▲) and (**A**; R = Ph, R′ = Et) (●). Experimental data are shown in Table 11, measured in tetrahydrofuran at 25.0 °C

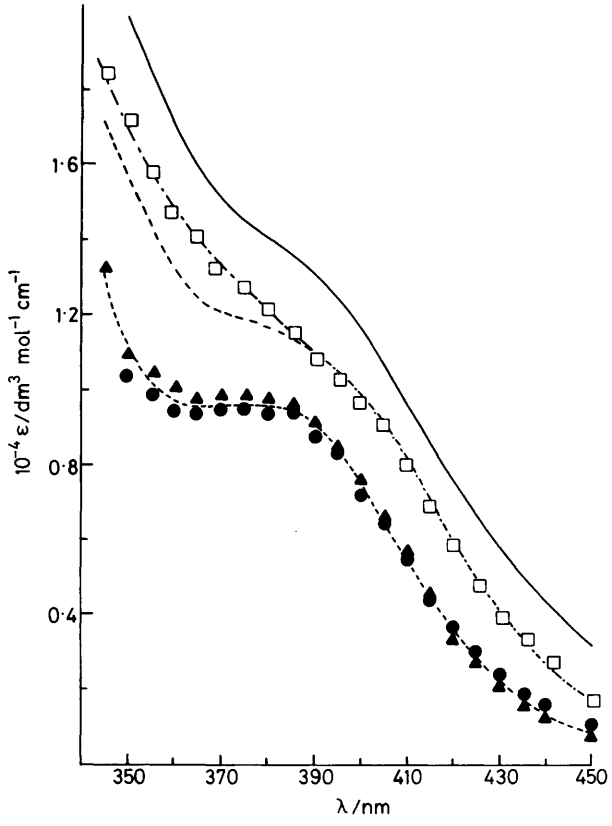

Figure 9. Visible spectra of complexes (**A**; R = R′ = Me) (—), (**D**; R = R′ = Me) (– – –), and the equilibrium mixture of (**B**) and (**C**) (R = R′ = Me) measured at [HCl] = 25.0 mmol dm^{-3} (▲) and [HBr] = 0.5 mmol dm^{-3} (●), in tetrahydrofuran. Also shown is the spectrum of (**H**; R = R′ = Me) (□) measured in 5.0 mmol dm^{-3} NEt_2H

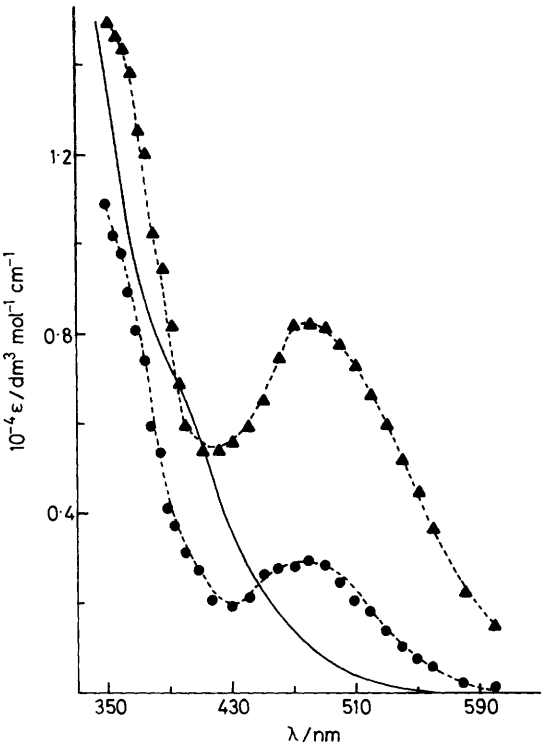

Figure 10. Visible spectra of complex (**A**; R = Ph, R′ = Et) (—) and of the detected species (**B**) (▲) and (**D**) (●) measured at [HCl] = 100.0 mmol dm^{-3} in tetrahydrofuran

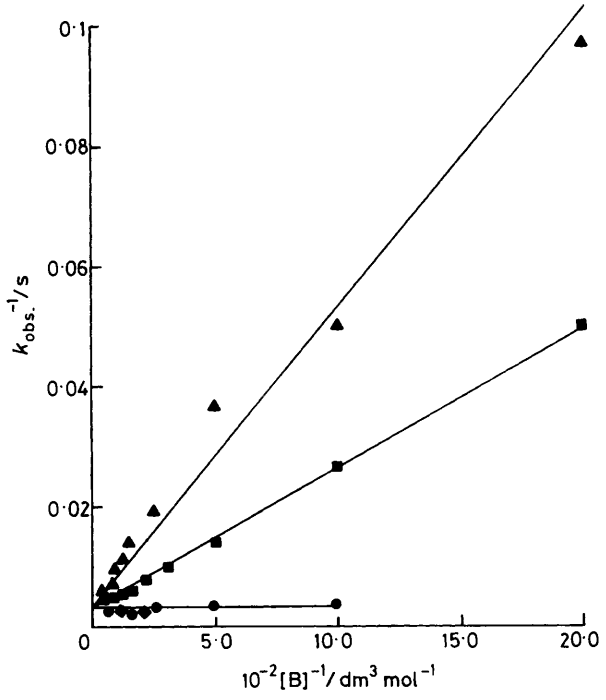

Figure 11. Graph of $1/k_{obs.}$ against 1/[B] where B = NEt_3 (▲), NBu^n_3 (■), NEt_2H (●), or $[NEt_4]Cl$ (◆) for the reactions of base with complex (**D**; R = R′ = Me) in tetrahydrofuran at 25.0 °C and 0.1 mol dm^{-3} $[NBu_4]BF_4$

of the acid concentration. The rate of this reaction is unperturbed by deuterium labelling of the acid, and the presence of $[NEt_4]Cl$ as shown in Table 10. The rate of the reaction of (**D**) with HCl [$k_{obs.}$ = (2.9 ± 0.3) × 10^{-3} s^{-1}] is identical to that observed for one phase of (**A**; R = R′ = Me).

The reaction of an excess of base B (NEt_3, NEt_2H, NBu^n_3, or Cl^-) with (**D**) rapidly gives the parent hydrazido(2−)-complex (**A**) as shown in equation (6).

$$[Mo(NHNMePh)(NNMePh)(S_2CNMe_2)_2]^+ + B \longrightarrow cis\text{-}[Mo(NNMePh)_2(S_2CNMe_2)_2] + HB^+ \quad (6)$$

The reaction of complex (**D**) with $[NEt_4]Cl$ or NEt_2H occurs in two phases: an initial rapid reaction, complete within the dead-time of the stopped-flow apparatus ($k_{obs.}$ > 300 s^{-1}), followed by the relatively slow reaction resulting in the production of (**A**). The rate of the slow phase exhibits a first-order dependence upon the concentration of (**D**), but is independent of the concentration and nature of the base ($k_{obs.}$ = 260 ± 20 s^{-1}), as shown in Table 12.

The reaction of complex (**D**) with the tertiary amines, NEt_3 or NBu^n_3, is complicated. The kinetics of either reaction exhibits a non-linear dependence on the concentration of base as shown in Table 12 and Figure 11. Furthermore, the rate of the reaction with NEt_3 is unperturbed by the presence of NEt_3H^+. The generalised rate expression observed in the reactions with the tertiary amines is shown in (7). When R = Et, a =

$$k_{obs.} = \frac{a[NR_3]}{1 + b[NR_3]} \quad (7)$$

(2.1 ± 0.1) × 10^4 dm^3 mol^{-1} s^{-1}, b = 80.8 ± 2.2 dm^3 mol^{-1}, and when R = Bu^n, a = (4.4 ± 0.2) × 10^4 dm^3 mol^{-1} s^{-1}, b = 170.9 ± 25 dm^3 mol^{-1}. At high concentrations of base the limiting rate constant is identical to that observed with the other bases ($k_{obs.}$ = 250 ± 10 s^{-1}). Under these conditions the time course is identical to that observed with $[NEt_4]Cl$ or NEt_2H.

Discussion

The reactions summarised in the Scheme readily rationalise the results of the kinetic studies. They will be discussed in two sections: the studies on the protonation of complexes (**A**) to form substituted hydrazines, and the deprotonation studies on (**D**).

The Mechanism of Formation of Hydrazines.—Protonation of complexes (**A**) occurs initially on one of the hydrazido(2−)-ligands, at the nitrogen atom adjacent to the metal (N_α), irrespective of the substituents on the remote nitrogen atom (N_β). This produces (**B**) containing the end-on hydrazido(1−)-ligand. The equilibrium constants for this protonation (K_1^{Me} = 120 ± 5 and K_1^{Ph} = 75 ± 3 dm^3 mol^{-1}) are reasonably insensitive to the nature of the substituents on N_β, consistent with this interpretation. It is not possible to measure the rate of this protonation, from these studies, but a lower limit of k_1 > 1 × 10^6 dm^3 mol^{-1} s^{-1} can be estimated. Thus, despite the conjugated nature of the hydrazido(2−)-ligand, protonation still occurs relatively rapidly. However, the complexes (**A**) differ somewhat from many hydrazido(2−)-complexes in that they are formally 20-electron species, containing an incipient lone pair on N_α, and therefore this ready protonation of N_α may not be so marked in co-ordinatively saturated complexes.

At all concentrations of HCl, diprotonation of complex (**B**; R = R′ = Me) occurs (K_2^{Me} = 140 ± 20 dm^3 mol^{-1}, Figure 7). There are three positions where this second protonation can occur: the metal, the remaining hydrazido(2−)-ligand, or N_β of

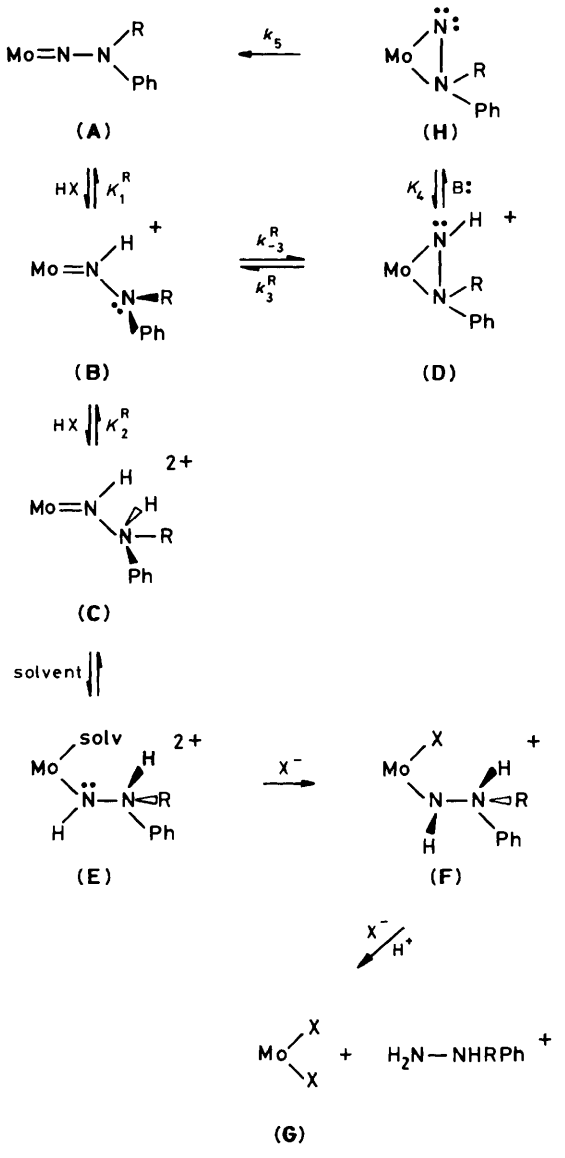

Scheme. Coligands have been omitted for clarity. Complexes (**A**), (**D**; R = Ph, R′ = Et), and (**G**; X = Cl) have been isolated, and (**B**), (**C**; R = R′ = Me) and (**H**; R = R′ = Me) have been detected spectrophotometrically

the hydrazido(1−)-residue [studies with (**D**; R = R′ = Me) demonstrate that this second protonation does not occur on this NN′-bonded species]. It is concluded that the correct formulation is shown in (**C**). The substituents on N_β act as a probe for this protonation. In contrast to the results with (**A**; R = R′ = Me), for the complex (**A**; R = Ph, R′ = Et) an upper limit of $K_2^{Ph} < 1.5$ dm^3 mol^{-1} can be estimated. This difference in acidities of complex (**C**; R = R′ = Me) and (**C**; R = Ph, R′ = Et) parallels the pK_a values of $NMePhH_2^+$ (4.8)[17] and $NPh_2H_2^+$ (*ca.* 0.8).[18]

It is interesting that the values of K_1^{Me} and K_2^{Me} are comparable despite the more unfavourable charge on complex (**B**). Presumably this is a consequence of the initial protonation at N_α promoting a second protonation at N_β. It is not entirely clear why one of the hydrazido (2−)-ligands acts as a 'spectator' during these reactions, but presumably protonation at N_α of one ligand withdraws electron density from the metal, thus decreasing the basicity of the remaining hydrazido(2−)-ligand. Furthermore the co-ordinatively saturated nature of (**B**) renders protonation at ligating atoms energetically more demanding.

Rapid ring closure of the hydrazido(1−)-ligand to form complex (**D**), containing the side-on, NN′-co-ordinated hydrazido(1−)-ligand, can compete with protonation of (**B**), as demonstrated by the isolation of (**D**; R = R′ = Me) at low acid concentrations.[9] The biphasic absorbance–time curves observed in the reactions of complex (**A**; R = R′ = Me) can be attributed to this competition. Thus after the rapid establishment of the equilibria between (**A**), (**B**), and (**C**), ring closure yielding (**D**) and the formation of hydrazine from (**C**) occur at comparable rates [$k_{obs.} = (1.6 \pm 0.2) \times 10^{-2}$ s^{-1}]. The slow phase of the reaction between complex (**A**) and HCl occurs at a rate identical to that of the reaction of (**D**; R = R′ = Me) with HCl [$k_3 = (2.9 \pm 0.3) \times 10^{-3}$ s^{-1}]. The kinetic studies on the protonation of (**D**) indicate that slow ring opening is essential to 'activate' the hydrazido(1−)-residue, and in this sense the side-on configuration is only 'enforced' in the present system.

The hydrazine-forming pathway involves attack of solvent on (**C**) to generate the species (**E**), in which the hydrazide ligand adopts the configuration shown to retain the 18-electron count for this species. Subsequent substitution of the solvent by the more electron-releasing halide renders the hydrazide ligand sufficiently basic for further protonation to occur to yield (**F**). Dissociation of the hydrazine, and rapid attack by halide, yields the product, $[MoX_2(NNRPh)(S_2CNR'_2)_2]$ (**G**). The kinetics of the decomposition of complex (**C**) is consistent with either rate-limiting attack of tetrahydrofuran (thf) on (**C**), or the subsequent dissociation of the solvent from (**E**) [R = R′ = Me, $k_{obs.} = (1.6 \pm 0.2) \times 10^{-2}$ s^{-1}]. Attempts to probe further the important role played by the solvent in this mechanism were made using the sterically hindered derivative of thf, 2,5-dimethyltetrahydrofuran. Although this substitution has been used successfully to probe the role of the solvent in other studies, its poor solvating properties in respect of both complex (**A**) and $[NBu_4]BF_4$ precludes its use in the present system.

It is proposed that the reaction of complex (**A**; R = Ph, R′ = Et) with acid proceeds in an analogous fashion to that described for (**A**; R = R′ = Me). In contrast to the studies described above, only monoprotonation of (**A**; R = Ph, R′ = Et) can be detected ($K_1^{Ph} = 75 \pm 3$, $K_2^{Ph} < 1.5$ dm^3 mol^{-1}). Ring closure of the hydrazido(1−)-residue in (**B**) ($k_{-3}^{Ph} = 0.51 \pm 0.05$ s^{-1}) yields (**D**) whose spectrum is shown in Figure 10. The steric and electronic influences of the phenyl substituents result in the faster ring opening of (**D**; R = Ph, R′ = Et) [$k_3^{Ph} = (1.5 \pm 0.3) \times 10^{-2}$ s^{-1}], compared to that observed with (**D**; R = R′ = Me), prior to the formation of Ph_2NNH_2, presumably *via* the pathway (**C**) to (**G**), although in this case a more direct route from (**B**) to (**G**) is conceivable.

The assignments of k_3^{Ph} and k_{-3}^{Ph} are not unambiguous[19] because of the identical kinetic orders of both phases of the reaction between complex (**A**; R = Ph, R′ = Et) and HCl, and the absence of an independently studiable (**D**) (a consequence of the faster ring-opening reaction of this species).

The Side-on NN′-Bonded Hydrazido(2−)-ligand.—Deprotonation of complex (**D**; R = R′ = Me) with a variety of bases results in the transient formation of (**H**) prior to the rapid ($k_5 = 260 \pm 20$ s^{-1}) ring-opening reaction to yield (**A**). The time course of this reaction is dependent upon the base. Only when the base is NEt_2H or Cl^-, or at high concentrations of the tertiary base, can the species (**H**) be detected spectroscopically. At low concentrations of NR_3 (R = Et or Bu^n) the observed rate equation is as shown in (7), and the initial absorbance corresponds to that of complex (**D**). This kinetic behaviour is not a consequence of the inextensive deprotonation of (**D**) by these bases since $[NEt_3H]BPh_4$ has no effect on the rate of the reaction with NEt_3. Furthermore NEt_3H^+ and $NEt_2H_2^+$ have

very similar aqueous pK_a values (10.7 and 11.0 respectively),[18] but markedly different behaviour with (**D**), and the less basic $NBu^n_3H^+$ (pK_a = 9.9)[18] also exhibits 'saturation kinetics' in its reaction with (**D**). It is proposed, therefore, that the observed kinetics results from low association constants for the more hindered tertiary amines with (**D**), prior to the rapid deprotonation step as shown in equation (8). The derived

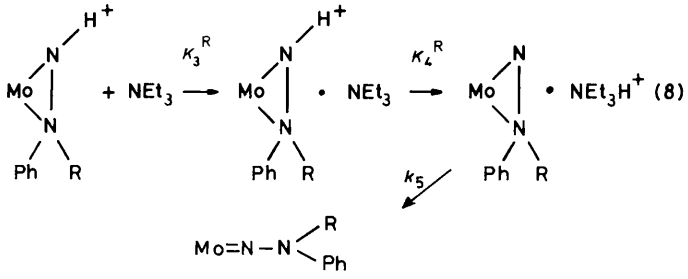

generalised rate expression for the conversion of complex (**D**) to (**A**) is thus that shown in (9), assuming that the value of $K_4 \gg 1$.

$$k_{obs.} = \frac{K_3^R K_4^R k_5[\mathbf{B}]}{1 + K_3^R K_4^R[\mathbf{B}]} \quad (9)$$

When B = NEt_2H or Cl^-, and at high concentrations of NR''_3 (R'' = Et or Bu^i), $K_3^R K_4^R[B] \gg 1$ and $k_{obs.} = k_5 = 250 \pm 10$ s^{-1}. At lower concentrations of NR''_3, $k_{obs.} = K_3^R K_4^R k_5[NR''_3]$, where $K_3^R K_4^R = 80.8 \pm 2.2$ (R'' = Et) and $K_3^R K_4^R = 170.9 \pm 7.5$ dm^3 mol^{-1} (R'' = Bu^n). A lower limit can be estimated for the values of $K_3^R K_4^R$ (B = NEt_2H or Cl^-) of $> 1 \times 10^3$ dm^3 mol^{-1}.

Although several complexes, such as $[W(\eta^5\text{-}C_5H_5)_2(NHNHR)H]$ (R = aryl)[20] and $[TiCl_2(\eta^5\text{-}C_5H_5)(NMeNMePh)]$,[12] as well as those described in this paper, containing the side-on hydrazido(1−)-ligand have been prepared, and the unique side-on, diazenido-complex $[TiCl_2(\eta^5\text{-}C_5H_5)(NNPh)]$[12] is also known, it is only in the present study that a hydrazido(2−)-ligand with this side-on configuration has been detected.

One further interesting aspect of these studies is that the ring-opening reaction of the hydrazido(1−)-ligand is relatively slow [$k_3^{Me} = (2.9 \pm 0.3) \times 10^{-3}$, $k_3^{Ph} = 1.5 \times 10^{-2}$ s^{-1}], whereas the ring opening of the analogous hydrazido(2−)-species is rapid ($k_5 = 260 \pm 20$ s^{-1}). This difference in reactivity is probably a consequence of the former reacting *via* a 16-electron intermediate, whereas the latter proceeds *via* a lower-energy 18-electron species.

Experimental

All reactions and manipulations were routinely performed under dinitrogen using standard Schlenk and syringe techniques as appropriate. The complexes *cis*-$[Mo(NNRPh)_2(S_2CNR'_2)_2]$ (R = Me or Ph, R' = Et),[8] $[Mo(NHNMePh)(NNMePh)(S_2CNMe_2)_2]BPh_4$,[9] and $[Mo(NHNHCO_2Me)(N_2COMe)(S_2CNMe_2)_2]$[10] were prepared by the literature methods. Tetrabutylammonium chloride (Lancaster synthesis), triethylamine, tributylamine, and diethylamine (B.D.H.) were used as supplied.

Stock solutions of anhydrous HCl were prepared in thf by the addition of equivalent amounts of $SiMe_3Cl$ and MeOH, and solutions of ^2HCl were prepared analogously using MeO^2H. Stock solutions were analysed by dilution with water, and then titrated against standard sodium hydroxide solution using phenolphthalein as indicator. Solutions of acid were used within 30 min of preparation. Solutions of anhydrous HBr were prepared similarly using equimolar concentrations of $SiMe_3Br$ and MeOH, and were used within 5 min of preparation.

Triethylammonium tetraphenylborate, $[NEt_3H]BPh_4$.—Triethylammonium chloride (2.0 g) was dissolved in methanol (10 cm^3) and sodium tetraphenylborate (5.2 g) dissolved in methanol (10 cm^3) was slowly added dropwise. The white solid was removed by filtration, washed with water to remove sodium chloride, then methanol and diethyl ether, and finally dried in air (Found: C, 85.9; H, 8.2; N, 3.1. Calc. for $C_{30}H_{36}BN$: C, 85.5; H, 8.6; N, 3.3%).

Dichlorobis(dimethyldithiocarbamato)[N'-methyl-N'-phenylhydrazido(2−)]molybdenum(VI), $[MoCl_2(NNMePh)(S_2CNMe_2)_2]$.—The complex $[Mo(NNMePh)_2(S_2CNMe_2)_2]$ (0.5 g) was suspended in methanol and $SiMe_3Cl$ (0.5 cm^3) added. The resulting solution was stirred for 0.5 h, evaporated to dryness, and the residue titrated with diethyl ether (30 cm^3) to give a yellow-orange solid (0.32 g, 70%).

The complex $[MoCl_2(NNPh_2)(S_2CNMe_2)_2]$ was prepared analogously in 77% yield.

[Benzoylhydrazido(1−)][benzoylhydrazido(2−)]dichlorobis(triphenylphosphine)rhenium(V), $[ReCl_2(NHNHCOPh)(NNHCOPh)(PPh_3)_2]$.—The complex $[ReCl_2(N_2COPh)(PPh_3)_2]$ (0.5 g, 0.54 mmol) and benzoylhydrazine (0.5 g, 3.6 mmol) were heated under reflux in methanol (40 cm^3) for 2 h. On cooling the complex deposited as a grey-green solid which was recrystallised as small prisms (0.33 g, 55.5%) from dichloromethane–diethyl ether.

Kinetic Studies.—All rapid reactions ($t_{\frac{1}{2}} < 30$ s) were studied on an Aminco-Morrow stopped-flow apparatus, modified to handle air-sensitive solutions as described before.[6] The apparatus was interfaced to a B.B.C. micro-computer (Acorn Computers, Cambridge) *via* an analogue-to-digital converter, operating at 3 kHz. Data were subsequently transferred to a PDP 1134A computer for analysis. Biphasic absorbance–time traces were fitted with two exponentials using a least-squares program, NAG subroutine EO4 5BF. For slower reactions the output of the photomultiplier unit was connected directly to an XY/t recorder (JJ instruments, model PL4), and the absorbance–time trace analysed by the normal methods.[19]

The reaction of $[Mo(NHNMePh)(NNMePh)(S_2CNMe_2)_2]BPh_4$ with HCl was studied on a SP1800 Pye Unicam spectrophotometer equipped with a thermostatted cell holder. Thermostatted water was circulated from a Grants thermostat tank (SE10).

X-*Ray Structural Studies.*—The *X*-ray studies were carried out as described in Table 1 and ref. 8.

Acknowledgements

The skilled technical assistance of Mr. F. O'Flaherty is gratefully acknowledged. We are also greateful to Professor M. Truter and Dr. D. L. Hughes of AFRC Rothamstead for the collection of an *X*-ray crystallographic data set.

References

1 R. A. Henderson, G. J. Leigh, and C. J. Pickett, *Adv. Inorg. Chem. Radiochem.*, 1983, **27**, 197 and refs. therein.
2 R. N. F. Thornley, R. R. Eady, and D. J. Lowe, *Nature (London)*, 1978, **272**, 557.
3 J. Chatt, R. A. Head, G. J. Leigh, and C. J. Pickett, *J. Chem. Soc., Dalton Trans.*, 1978, 1638.
4 J. Chatt, W. Hussain, G. J. Leigh, H. Neukomm, C. J. Pickett, and D. A. Rambin, *J. Chem. Soc., Chem. Commun.*, 1972, 1010.

5 S. N. Anderson, M. E. Fakeley, R. L. Richards, and J. Chatt, *J. Chem. Soc., Dalton Trans.*, 1981, 1973.
6 R. A. Henderson, *J. Chem. Soc., Dalton Trans.*, 1982, 917.
7 R. A. Henderson, *J. Chem. Soc., Dalton Trans.*, 1984, 2259.
8 J. Chatt, B. A. L. Crichton, J. R. Dilworth, P. Dahlstrom, R. Gutkoska, and J. A. Zubieta, *Inorg. Chem.*, 1983, **21**, 2383.
9 J. Chatt, J. R. Dilworth, P. Dahlstrom, and J. A. Zubieta, *J. Chem. Soc., Chem. Commun.*, 1980, 786.
10 J. R. Dilworth and J. A. Zubieta, *Transition Met. Chem.*, 1984, **9**, 39.
11 T. Nicholson and J. A. Zubieta, *J. Chem. Soc., Chem. Commun.*, 1985, 367.
12 J. R. Dilworth, I. A. Latham, G. J. Leigh, G. Hüttner, and I. Jibril, *J. Chem. Soc., Chem. Commun.*, 1983, 1368.
13 J. A. McCleverty, A. E. Rae, I. Wolockowicz, N. A. Bailey, and J. M. A. Smith, *J. Chem. Soc., Dalton Trans.*, 1983, 71.
14 J. R. Dilworth, S. A. Harrison, D. R. M. Walton, and E. Schweda, *Inorg. Chem.*, 1983, **24**, 2594.
15 T. A. George, G. E. Bossard, D. B. Howell, L. M. Koczon, and R. K. Lester, *Inorg. Chem.*, 1983, **22**, 1968.
16 S. Fried and R. D. Keene, *J. Am. Chem. Soc.*, 1941, **63**, 2691.
17 N. F. Hall and M. R. Sprinkle, *J. Am. Chem. Soc.*, 1982, **54**, 3469.
18 F. M. Jones and E. M. Arnett, *Prog. Phys. Org. Chem.*, 1974, **11**, 263.
19 J. M. Espenson, 'Chemical Kinetics and Reaction Mechanisms,' McGraw-Hill, New York, 1981, ch. 2.
20 J. A. Carroll and D. Sutton, *Inorg. Chem.*, 1980, **19**, 3137.

Received 10*th April* 1986; *Paper* 6/704